 CMES, vol.24, no.1, pp.61-80, 2008

# A stabilized RBF collocation scheme for Neumann type boundary value problems

**Nicolas Ali Libre[1,2], Arezoo Emdadi[2], Edward J. Kansa[3,4], Mohammad Rahimian[2], Mohammad Shekarchi[2]**

**Abstract:** The numerical solution of partial differential equations (PDEs) with Neumann boundary conditions (BCs) resulted from strong form collocation scheme are typically much poorer in accuracy compared to those with pure Dirichlet BCs. In this paper, we show numerically that the reason of the reduced accuracy is that Neumann BC requires the approximation of the spatial derivatives at Neumann boundaries which are significantly less accurate than approximation of main function. Therefore, we utilize boundary treatment schemes that based upon increasing the accuracy of spatial derivatives at boundaries. Increased accuracy of the spatial derivative approximation can be achieved by h-refinement reducing the spacing between discretization points or by increasing the multiquadric shape parameter, c. Increasing the MQ shape parameter is very computationally cost effective, but leads to increased ill-conditioning. We have implemented an improved version of the truncated singular value decomposition (IT-SVD) originated by Volokh and Vilnay (2000) that projects very small singular values into the null space, producing a well conditioned system of equations. To assess the proposed refinement scheme, elliptic PDEs with different boundary conditions are analyzed. Comparisons that made with analytical solution reveal superior accuracy and computational efficiency of the IT-SVD solutions.

**Keyword:** meshfree, multiquadric, RBF collocation, strong form, Neumann condition, stability, boundary value problem, improved truncated singular value decomposition.

[1] Corresponding author, nalibre@ut.ac.ir
[2] Department of civil Engineering, University of Tehran, Tehran, Iran
[3] Corresponding author, ejkansa@ucdavis.edu
[4] Department of Mechanical and Aeronautical Engineering, University of California, Davis, CA 95616 USA

## 1 Introduction

The drawback of mesh-based computational methods for the simulation of problems with extremely large deformations, complex geometry, or moving discontinuities is that frequent remeshing is required. Such problems have motivated many researchers to develop the so-called meshfree methods that do not depend on meshes or grids.

Multiquadric (MQ) radial basis functions (RBFs) are a type of node-based approximation scheme that was devised by the geo-physical engineer, Hardy (1971, 1990), who worked on scattered data fitting and general multi-dimensional data interpolation problems. Madych and Nelson (1988, 1990) and Buhmann and Micchelli (1990) have shown theoretically that the MQ-RBF approximation scheme converges faster as the spatial dimension, discretization and MQ shape parameters are refined. Numerically, Fedoseyev, Friedman, and Kansa (2002), Cheng, Golberg, Kansa and Zammito (2003), Huang, Lee, and Cheng (2007), Fornberg, and Driscoll (2002), Fornberg and Wright (2004), and Fornberg, Wright, and Larsson (2004), demonstrated that the solution of elliptic PDEs using radial basis functions converge exponentially. Recently, Young, Chen, and Wong (2005) demonstrated the successful application of the MQ method in the solution of Maxwell's equations in two and three dimensions.

Although MQ-RBFs enjoy superior convergence rates, the present principal disadvantage of solving PDE systems by MQ-RBF collocation method is that the resulting equation system can become

quickly ill-conditioned as the number of nodes increases. This ill-conditioning hinders applicability of the RBF collocation method to large scale engineering problems where many nodes are required for proper mathematical modeling of complex physical phenomena. In order to bypass the ill-conditioning associated with the global RBFs, Sarler (2005) and Tolstykh and Shirobokov (2005) developed an RBF analog of finite differences to obtain a compactly supported scheme with convergence rates superior to polynomial based finite differences, but less than the global RBF scheme , verifying the Schaback (1995) trade-off principle.

Although several authors such as: Kansa and Hon (2000), Ingber, Chen, and Tanski (2004), Ling and Kansa (2004), and Adibi and Es'haghi (2007) have demonstrated that domain decomposition has the advantage of breaking a very large problem in many smaller sub problems that have vastly improved conditioning, many researchers are apparently hesitant in applying domain decomposition, in spite of the fact that domain decomposition is widely used in complex problems in which finite difference, finite element, or finite volume methods are employed.

Another reason that people ignore RBF methods is that the Neumann boundary conditions are poorly behaved and may result in enormous errors at or near Neumann boundaries. Therefore an accurate and stable solution method for boundary value problems with Neumann boundary conditions is much more difficult to obtain than that with Dirichlet boundary conditions. The ill-conditioning nature of the equation system in the direct RBF collocation method intensifies the difficulty of imposing Neumann boundary conditions. As a consequence, there has been interest in trying to find a treatment technique for imposing the Neumann boundary condition that bypasses the ill-conditioning problem of the RBF collocation methods.

Zhang, Song, Lu, and Liu (2000) pointed out that the poor accuracy of Neumann boundary conditions is due to the poor quality of the derivative approximations on the boundary. Based on this fact, they proposed the Hermite type collocation method in which both PDEs and prescribed traction boundary conditions are imposed on the natural boundary. Liu and Gu (2003) noticed that Neumann conditions are well posed in the weak form based numerical methods. By considering the fact that in meshfree collocation methods, instability and computational errors are mainly induced by the Neumann boundary conditions, Liu and Gu (2003) proposed the meshfree weak-strong (MWS) form in which the collocation is used for all nodes whose local quadrature domains do not intersect the Neumann boundaries, while the local weak form is used only for nodes on or near natural boundaries. The reason for the better performance is due to integration of the normal partial derivatives since anti-differentiation increases the convergence rate following the analysis of Madych (1992).

Hu, Chen, and Hu (2006) proposed the weighted RBF collocation method for boundary value problems. They observed that the error analysis shows there are unbalanced errors among the domain, Neumann boundary, and Dirichlet boundary terms. These unbalanced errors are treated by introducing proper scaling weight for the Neumann and Dirichlet boundary collocation equations.

Motivated by the aforementioned work, we are interested in stabilizing the RBF collocation scheme for boundary value problem subjected to mixed Neumann and Dirichlet boundary conditions. The work presented herein focuses on the utilization of boundary treatment schemes together with a stable solver of severely ill-conditioned equation systems to mitigate the instabilities of the RBF collocation scheme.

## 2 Solving PDEs by direct RBF collocation method

Consider $\mathscr{L}$ to be a differential operator that is defined on d-dimensional simply connected domain, $\Omega \subseteq \Re^d$ with a piecewise smooth boundary,$\partial\Omega$. The general form of boundary value problem is defined in Eq (1-3).

$$\mathscr{L}\mathrm{u}=\mathscr{F} \text{ in } \Omega\backslash\partial\Omega \tag{1}$$

$$\mathrm{u}=\mathrm{u}^* \text{ on } \partial\Omega^{\mathrm{u}} \tag{2}$$

ßu=t* on $\partial\Omega^{t}$ (3)

where $\partial\Omega^{t}$ is the natural boundary with Neumann condition and $\partial\Omega^{u}$ is the essential boundary with Dirichlet condition. In order to solve the above problem, we need to find a function u(**X**) that satisfies the governing differential operator $\mathscr{L}$ in the interior domain, $\Omega\backslash\partial\Omega$, the Dirichlet boundary condition on the essential boundary, $\partial\Omega^{u}$, and the Neumann boundary condition on the natural boundary, $\partial\Omega^{t}$. Given an unknown function u(**X**):$\Re^{d} \rightarrow \Re$ and N distinct source points S=$\{\mathbf{X}_j\}_{j=1}^{N} \in(\Omega \cup \partial\Omega) \subset \Re^{d}$ the unknown function, u(**X**), is interpolated in terms of a series of known RBFs multiplied by an unknown set,$\{\alpha\}$, of expansion coefficients.

$$u(\mathbf{X}) = \sum_{j=1}^{N} \varphi(\mathbf{X}\text{-}\mathbf{X}_j)\alpha_j = \sum_{j=1}^{N} \varphi_j(\mathbf{X})\alpha_j \tag{4}$$

where $r_j=||\mathbf{X}\text{-}\mathbf{X}_j||$ is the Euclidian norm, $\varphi_j$ are the radial basis functions, and $\alpha_j$ are the coefficients to be determined. Most widely used global radial basis functions are the multiquadric (MQ) $\varphi_j=(r_j^2+c_j^2)^{1/2}$, the Gaussian $\varphi_j=\exp(-(r_j/c_j)^2)$, and the thin plate spline (TPS) $\varphi_j= r_j^2\log(r_j)$, where $c_j$ is the shape parameter. An important advantage of the MQ and Gaussian RBFs is that these commonly used global RBFs are infinitely differentiable. Therefore, spatial derivatives of the function u(**X**) up to desired degree,n, could be obtained as below:

$$\frac{\partial^{n} u}{\partial X^{n}}(\mathbf{X}) = \sum_{j=1}^{N} \frac{\partial^{n}\varphi_j(\mathbf{X})}{\partial X^{n}}\alpha_j \tag{5}$$

The continuous boundary value problem of Eqs (1-3) can be approximately transformed into a system of simultaneous algebraic equations by substituting the expressions of the unknown function u(X) and its derivatives into Eqs (1-3) and collocating the governing equation and boundary conditions on a set of m distinct collocation points. The accuracy of the boundary value problem using collocation scheme depends upon the accuracy of the approximating PDE and the corresponding BCs on the collocation points in the domain and on the boundary, respectively. The most arguable issue of collocation based meshfree methods is the poor implementation of Neumann BCs due to the poor approximation of spatial derivatives on the boundary. In any approximation method, approximations of spatial derivatives are less accurate because differentiation reduces the order of the approximation. Even though MQ-RBF enjoys spectral convergence of order, $O(\lambda^{\mu})$, where $\mu$ = (c/h), and $0 < \lambda < 1$, Madych (1992) clearly shows spatial derivatives of order, $\varsigma$, reduce their convergence rates to $O(\lambda^{\mu-|\varsigma|})$. There are several options available to increase the convergence rates of spatial derivatives of MQ-RBFs. They are:

1. Increase $\mu$ by increasing c and/or decreasing h, so $\mu >> \varsigma$.

2. Anti-differentiation (integration) methods of Mai-Duy and Tran-Cong (2003, 2007) increase the order of successive derivatives to off-set the reduction of convergence rate given by Madych's estimate.

3. Instead of using the usual MQ or IMQ basis function, $\varphi_j = (r_j^2+c_j^2)^{(1/2)}$ or $\varphi_j= (r_j^2+c_j^2)^{(-1/2)}$ respectively, one should consider a higher order MQ function such as $\varphi_j = (r_j^2+c_j^2)^{\beta}$ where $\beta >$ (1/2). Wertz, Kansa, and Ling(2006) showed that for $\beta$ ranging from 3/2 to 11/2, the MQ basis function becomes increasingly flatter near the point, $\mathbf{X}_j$ and the derivative of such higher order functions appears to be better behaved.

Let $C_d$ be a set of $m_d$ collocation points in $\Omega$, $C_t$ be a set of $m_t$ collocation points on $\partial\Omega^{t}$, and $C_u$ be a set of $m_u$ collocation points on $\partial\Omega^{u}$. Generally, the source points and the collocation points $C=\{\mathbf{X}_j\}_{j=1}^{m}= C_d \cup C_t \cup C_u$ should not necessarily have shared points; but usually, the source points and the collocation points can coincide. By substituting the approximated solution in the strong form (1-3) and satisfying the differential and boundary operators at the collocation points, the continuous boundary value problem is approximately transformed to an algebraic discrete equation in the form of $\mathbf{A}\alpha = \mathbf{b}$. Clearly, there exists a unique solution if and only if **A** is non-singular. The non-singularity of **A** for certain classes of are discussed by Micchelli (1986) and Wendland (2005), using the fact that **A** is either strictly pos-

itive definite (IMQ, Gaussians), or strictly conditionally positive definite of order one for MQ and $\beta$=1/2. The set of equations is strictly conditionally positive definite that guarantees the non-singularity of the corresponding system matrix.

For numerical verification purpose we focus on solving the following elliptic operator that is usually known as Navier's equilibrium equations.

$$\mu\nabla^2 \mathrm{u} + (\lambda+\mu)\nabla(\nabla\cdot \mathrm{u}) + \mathbf{b} = 0 \quad \text{in } \Omega\backslash\partial\Omega \subseteq \Re^{\mathrm{d}},\ \mathrm{d}=1,2,\text{or } 3. \tag{6}$$

$$\mathrm{u} = \mathrm{u}^* \text{ on } \partial\Omega^{\mathrm{u}}, \tag{7}$$

$$\mathrm{t_i} = \mathrm{t_i}^* \text{ on } \partial\Omega^{\mathrm{t}}, \tag{8}$$

where u is displacement vector,and in this context, $\mu$ and $\lambda$ are Lame's constants, **b** is the body force, u* is the prescribed displacement on essential boundary, $\mathrm{t}_i=\sigma_{ij}\mathrm{n}_j$ is the ith component of the surface traction, and $\mathrm{t}_i$* is the ith component of the applied surface traction on the natural boundary. The solution of 2D elasticity problems is approximated by RBFs as below:

$$\mathbf{u} = (\mathrm{u_x}(\mathrm{x},\mathrm{y}),\mathrm{u_y}(\mathrm{x},\mathrm{y}))^{\mathrm{T}} \tag{9}$$

$$\mathrm{u_x}(\mathrm{x},\mathrm{y}) = \sum_{j=1}^{n} \varphi_{\mathrm{j}}(\mathrm{x},\mathrm{y})\alpha_{\mathrm{j}} \tag{10}$$

$$\mathrm{u_y}(\mathrm{x},\mathrm{y}) = \sum_{j=1}^{n} \varphi_{\mathrm{j}}(\mathrm{x},\mathrm{y})\beta_{\mathrm{j}} \tag{11}$$

By substituting Eq(9) into Eqs (6-8) and considering the 2D plane stress elasticity the following algebraic system is concluded. By substituting Eq (9) into Eqs (6-8) and considering the 2D plane stress elasticity the following algebraic system is obtained. Details are omitted here and can be found in Libre, Emdadi, Rahimian, and Shekarchi (2006).

$$\frac{\mathrm{E}}{1\text{-}\nu^2}\begin{pmatrix} \frac{\partial^2\varphi_{\mathrm{j}}}{\partial \mathrm{x}_1^2}+\frac{1-\nu}{2}\frac{\partial^2\varphi_{\mathrm{j}}}{\partial \mathrm{x}_2^2} & \frac{1+\nu}{2}\frac{\partial^2\varphi_{\mathrm{j}}}{\partial \mathrm{x}_1\partial \mathrm{x}_2} \\ \frac{1+\nu}{2}\frac{\partial^2\varphi_{\mathrm{j}}}{\partial \mathrm{x}_1\partial \mathrm{x}_2} & \frac{\partial^2\varphi_{\mathrm{j}}}{\partial \mathrm{x}_2^2}+\frac{1-\nu}{2}\frac{\partial^2\varphi_{\mathrm{j}}}{\partial \mathrm{x}_1^2} \\ \frac{1\text{-}\nu^2}{\mathrm{E}}\varphi_{\mathrm{j}} & 0 \\ 0 & \frac{1-\nu^2}{\mathrm{E}}\varphi_{\mathrm{j}} \\ \mathrm{n}_1\frac{\partial\varphi_{\mathrm{j}}}{\partial \mathrm{x}_1}+\mathrm{n}_2\frac{1-\nu}{2}\frac{\partial\varphi_{\mathrm{j}}}{\partial \mathrm{x}_2} & \mathrm{n}_1\nu\frac{\partial\varphi_{\mathrm{j}}}{\partial \mathrm{x}_2}+\mathrm{n}_2\frac{1-\nu}{2}\frac{\partial\varphi_{\mathrm{j}}}{\partial \mathrm{x}_1} \\ \mathrm{n}_1\frac{1-\nu}{2}\frac{\partial\varphi_{\mathrm{j}}}{\partial \mathrm{x}_2}+\mathrm{n}_2\nu\frac{\partial\varphi_{\mathrm{j}}}{\partial \mathrm{x}_1} & \mathrm{n}_1\frac{1-\nu}{2}\frac{\partial\varphi_{\mathrm{j}}}{\partial \mathrm{x}_1}+\mathrm{n}_2\frac{\partial\varphi_{\mathrm{j}}}{\partial \mathrm{x}_2} \end{pmatrix} \begin{bmatrix} \alpha_{\mathrm{j}} \\ \\ \beta_{\mathrm{j}} \end{bmatrix} = \begin{bmatrix} \mathrm{b}_1 \\ \mathrm{b}_2 \\ \mathrm{u}^*_1 \\ \mathrm{u}^*_2 \\ \mathrm{t}^*_1 \\ \mathrm{t}^*_2 \end{bmatrix} \tag{12}$$

Examples of authors using RBFs to solve solid mechanics problems are Lui and Gu (2003), Mai-Duy, Khennane, and Tran-Cong,(2006), Wen and Hon(2007), Ferreira, Roque, Jorge, and Kansa (2005).

## 3 Boundary treatment scheme

In the collocation procedure, the differential and boundary operators act upon the approximated solution at certain collocation points. So, the accuracy of the solution depends upon both the number of collocation points and the accuracy of the approximation at the collocation points. The numerical solution converges to exact solution by: (i) Increasing the number of collocation points so that the operators are satisfied at more regions in domain and on the boundary; (ii) Improving the accuracy of approximation so that the operators are more tightly satisfied at these collocation points.

In this section, we show numerically that the poor approximation of the spatial derivatives is the main error source in the imposition of the Neumann conditions on the natural boundary. For this purpose, we examine the accuracy of scattered data interpolation especially near and on the boundary. Consider a scattered data set in the form of ($\mathbf{X}_i$, $\mathrm{F}_i$) where the values of $\mathrm{F}_i$ are sampled from an arbitrary function F: $\Omega \subseteq \Re^d \rightarrow \Re$ at the source points S=$\{\mathbf{X}_j\}_{j=1}^n \in(\Omega \cup \partial\Omega) \subseteq \Re^d$. The

goal is to find an interpolation of the function F and its derivative up to desired degree in the form of Eq(5) and Eq(4) such that

$$F(\mathbf{X}_i) = \sum_{j=1}^{n} \varphi_j(\mathbf{X}_i)\alpha_j \tag{13}$$

The resulted linear equation system is solved using standard Gaussian elimination method to determine the unknown coefficients, $\alpha_j$. The maximum norm ($L_\infty$) as defined in Eq(13) is used to measure the solution accuracy.

$$L_\infty = max|F_i^h - F_i^{ex}| \tag{14}$$

where $F_i^h$ and $F_i^{ex}$ are the approximated and exact value, $u$,at the point, $\mathbf{X}_i$, respectively.

The accuracy of RBF interpolation is investigated through two numerical examples. Since the present examples are merely intended to explore the accuracy of approximation on the boundary, the error norm was also calculated in the domain and on the boundary, separately.

### 3.1 Test problem 1

A compatible 2D displacement field and the corresponding stress field that are usually used for the patch test analyses are given in Eq(15); these are considered here to compare the accuracy of approximating a linearly varying surface.

$$u_x = x,\ u_y = -y/4, \tag{15}$$

$$\sigma_{xx} = 1,\ \sigma_{xy} = 0,\ \sigma_{yy} = 0. \tag{16}$$

A uniform distribution of $6\times6$ points in the square domain $0\leq$ x, y $\leq5$ is used to sample the displacement field. The $L_\infty$error norms that are evaluated on a uniform distribution of $18\times18$ points are summarized in Table 1. Figure (1) shows the error distribution in $u_x$ and $\sigma_{xx}$ obtained by MQ RBF interpolation with c=3. This study shows that the MQ possess excellent accuracy in approximating the displacement field in the domain and on the boundary; but the accuracy of the stress field has deteriorated significantly on the boundary. Numerical results show that the $L_\infty$ errors in approximating the spatial derivatives of the stress field are significantly more than those of the displacement field. In addition, the accuracy of the stress fields is relatively decreased near and on the boundary.

### 3.2 Test problem 2

The displacement field of the plane stress cantilever beam problem subjected to an end shear force is considered as the second example. The displacement field and the corresponding stress fields are given in Eqs (16-19), and the problem is taken from Timoshenko and Goodier (1970).

$$u_x = \frac{-P}{6EI}(y-D/2)[(6L-3x)x+(2+\nu)(y^2-Dy)] \tag{17}$$

$$u_y = \frac{P}{6EI}[(3\nu(L-x)(y-\frac{D}{2})^2+\frac{(4+5\nu)}{4}xD^2+x^2(3L-x)\ ] \tag{18}$$

$$\sigma_{xx} = \frac{-P}{I}(L-x)(y-D/2);\ \ \sigma_{yy} = 0;\ \ \sigma_{xy} = \frac{Py}{2I}(y-D) \tag{19}$$

where $I=D^3/12$ is the moment of inertia , E is the Young's modulus, $\nu$ is the Poisson ratio, P is the applied force, and D and L are the height and length of beam respectively.

The displacement field is sampled in a uniform distribution of $19\times7$ points, then the displacement and stress field are approximated on $93\times33$ points that are uniformly distributed on the rectangle domain $0\leq$ x $\leq12$ and $0\leq$ y $\leq4$. The MQ RBF with a constant shape parameter, c=3, was used for interpolating the displacement and stress fields. The $L_\infty$ errors of approximation are given in Table 2. Figure (2) shows the error distribution of approximation.

Here again, the accuracy of the stress field approximation on the boundary is decreased significantly. In this problem, the error of approximating stress field on the boundary is substantially more than those in the patch test. Therefore, it is logically concluded that the analysis of cantilever beam problem is more sensitive to the Neumann

Table 1: $L_\infty$ error in scattered data fitting, test problem 1

| | $u_x$ | $u_y$ | $\sigma_{xx}$ | $\sigma_{yy}$ | $\sigma_{xy}$ |
|---|---|---|---|---|---|
| Domain | 0.7141E-2 | 0.1785E-2 | 1.0380E-2 | 0.3117E-2 | 0.2836E-2 |
| Boundary | 0.4828E-2 | 0.1207E-2 | 3.2855E-2 | 0.8786E-2 | 0.8099E-2 |

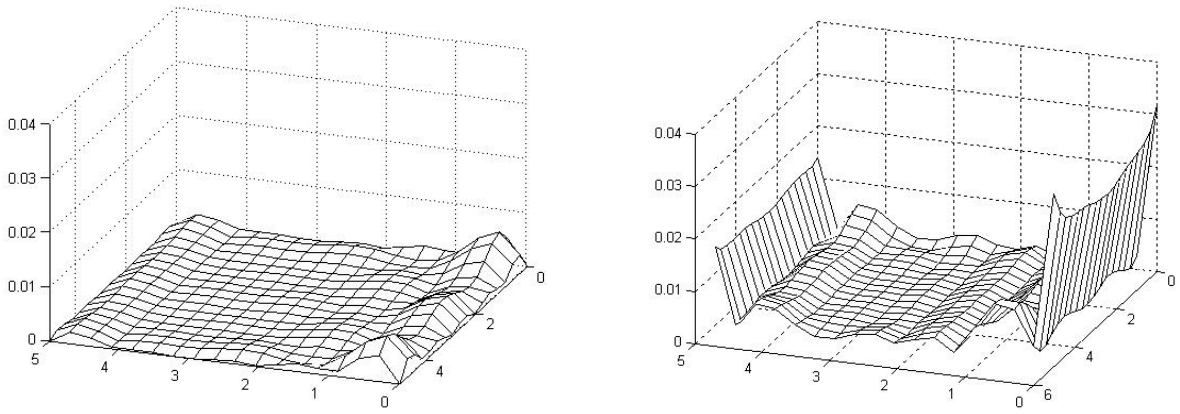


Figure 1: Error distribution in scattered data interpolation, test problem 1

Table 2: The $L_\infty$error in scattered data fitting, test problem 2

| | $u_x$ | $u_y$ | $\sigma_{xx}$ | $\sigma_{yy}$ | $\sigma_{xy}$ |
|---|---|---|---|---|---|
| Domain | 0.1836E-4 | 0.3921E-5 | 0.3380E-1 | 0.2015E-1 | 0.2652E-1 |
| Boundary | 0.1835E-4 | 0.4152E-5 | 1.2726E-1 | 0.7480E-1 | 0.6560E-1 |


(a) (b)

Figure 2: Error distribution in scattered data interpolation, test problem 2. (a)$u_x$ , (b) $\sigma_{xx}$

BCs than the patch test problem. The solution of cantilever beam problem subjected to Neumann BCs will be discussed in section 5.

Both of the above-presented numerical examples show the poor accuracy of stress field approximation on the boundary. In the point wise solution of boundary value problem using collocation procedure, the domain and boundary operators are satisfied on distinct points in domain and on boundary, respectively. The Dirichlet condition is well posed in the collocation procedure since the solution is well approximated on the boundary. But the poor approximation of the solution derivatives on the boundary reduces the accuracy of solving boundary value problems with Neumann BCs. The main source of instability emanating from Neumann BCs is the poor approximation of the function's derivative on the boundary. So, it is rational to conclude that any treatment scheme that based upon increasing the accuracy of approximating spatial derivatives on the boundary will reduce the instability arising from Neumann BCs in collocation based meshfree methods.

There are two ways to make the solution converge faster, either by refining the mesh size (h-scheme), or by increasing the shape parameter,

Table 3: $L_\infty$ error norm of approximating the stress filed on the boundary, test problem 1.

| h-scheme Data centers | h-scheme $\sigma_{xx}$ | h-scheme $\log_{10}$(cond) | c-scheme Shape parameter | c-scheme $\sigma_{xx}$ | c-scheme $\log_{10}$(cond) |
|---|---|---|---|---|---|
| 6×6 | 3.2855E-2 | 6.79 | 3 | 3.2855E-2 | 6.79 |
| 9×9 | 6.3581E-3 | 10.48 | 6 | 2.2848E-3 | 10.72 |
| 12×12 | 1.3595E-3 | 14.09 | 9 | 2.9813E-4 | 13.68 |
| 15×15 | * | 17.34 | 12 | 1.1401E-3 | 15.97 |
| 18×18 | * | 18.81 | 15 | * | 18.14 |

* Unstable solution due to round-off error

Table 4: $L_\infty$ error norm of approximating the stress filed on the boundary, test problem 2.

| h-scheme Data centers | h-scheme $\sigma_{xx}$ | h-scheme $\log_{10}$(cond) | c-scheme Shape parameter | c-scheme $\sigma_{xx}$ | c-scheme $\log_{10}$(cond) |
|---|---|---|---|---|---|
| 19×7 | 1.2726E-1 | 10.47 | 3 | 1.2726E-1 | 10.47 |
| 25×9 | 3.3474E-2 | 13.52 | 4 | 3.7756E-2 | 12.90 |
| 31×11 | * | 16.54 | 5 | 3.4535E-2 | 15.22 |
| 37×13 | * | 19.01 | 6 | * | 17.48 |

* Unstable solution due to round-off error

c (c-scheme). According to Madych (1992), if $\mu$=(c/h)>>$\varsigma$, then the loss on convergence by the differentiation approximation is small. While the h-scheme requires an increase of computational cost, the c-scheme is performed without extra CPU cost. The $L_\infty$ errors of the approximated stress field in the first and second test problems and the corresponding condition numbers of the coefficient matrixes schemes are listed in Table 3 and 4, respectively. In the h-scheme, the shape parameter was kept constant at c=3 in all analyses and the data centers were refined uniformly. In contrast, the c-scheme refinement is performed by increasing the shape parameter while a uniform 6×6 data center distribution was used for sampling.

The h-scheme is usually performed over a uniform grid but it is reasonable to allocate adaptively more centers to the boundary layer where a more accurate approximation is desired. Locating the centers near or on the boundary enables one to obtain more accurate results with a smaller number of additional centers. From our study we found that inserting centers near the boundary, as depicted in Figure (3), performs well.

In the same way, the c-scheme may be increased uniformly over the domain or it may be adaptively different over the interior and on the boundary. Wertz, Kansa, and Ling (2006) found that $c_{\partial\Omega} \approx 200 c_{\Omega\setminus\partial\Omega}$ performs the best in 2D Poisson problems. In our elasticity calculations, we chose $c_{\partial\Omega} \approx 1.5 c_{\Omega\setminus\partial\Omega}$ since the equation systems of RBF collocation in the elasticity problems are comparatively more ill-conditioned and the greater values of shape parameter cause numerical instabilities due to severe ill-conditioning.

Figure (4) and (5) shows the error distribution in the adaptive version of the h-scheme and c-scheme in the first and second test problem, respectively. The results of the adaptive refinement in test problem 1 and 2 are also summarized in Table 5 and 6, respectively.

The c-scheme is usually preferable to h-scheme since the h-scheme increases the rank of the coefficient matrix that leads to an increased expense in computer storage and CPU time. In contrast, the c-scheme can be performed without any extra computational cost. For purposes of efficiency, the c-scheme is superior and preferable over the h-scheme. In addition, the numerical results reveal the superiority of the adaptive h-scheme over the uniform h-scheme because the adaptive h-scheme requires many fewer data centers for convergence

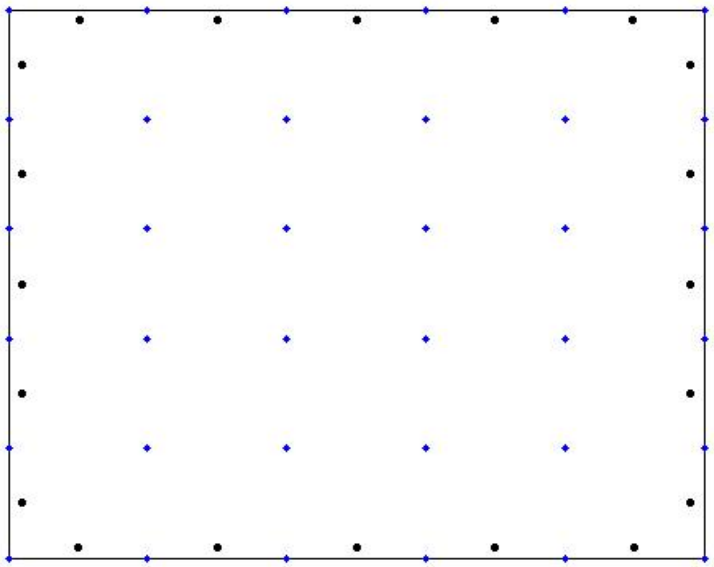

Figure 3: Adaptive node refinement by allocate more centers near the boundary layer

Table 5: Refining the approximation of $\sigma_{xx}$ stress filed on the boundary using adaptive h-scheme or adaptive c-scheme, test problem 1

| | Original solution | Refined solution Adaptive h-scheme | Refined solution Adaptive c-scheme |
|---|---|---|---|
| $L_\infty$ | 3.2855E-2 | 6.8341E-3 | 7.1814E-3 |
| CPU time (sec) | 1.1 | 1.7 | 1.2 |
| $\log_{10}$(cond) | 6.79 | 7.83 | 12.45 |

Table 6: Refining the approximation of $\sigma_{xx}$ stress field on the boundary using the adaptive h-scheme or adaptive c-scheme, test problem 2

| Adaptive scheme | Original solution | Refined solution Adaptive h-scheme | Refined solution Adaptive c-scheme |
|---|---|---|---|
| $L_\infty$ | 1.2726E-1 | 2.6099E-2 | 8.7866E-3 |
| CPU time (sec) | 37.9 | 50.7 | 42.5 |
| $\log_{10}$(cond) | 10.47 | 10.69 | 12.81 |

to the desired accuracy and a slower increase in ill-conditioning. The adaptive c-scheme is also superior to uniform c-scheme since the adaptive c-scheme produce more accurate results when the condition number was kept constant. Although the adaptive method performed suitably, in the rest of the paper, we use uniform schemes for treating Neumann BCs. But, we show the robustness of combined adaptive c-h scheme through a numerical example presented at the end of this paper. In the forthcoming paper we develop a new adaptive algorithm based on residual sampling to combine the adaptive c and h scheme for producing highly accurate results.

Obviously, an increasingly more accurate approximation of stress field on the boundary is obtained by the h and/or c scheme. But as a general principle, the better the approximation properties of the RBF collocation, the worse is its conditioning, see Schaback (1995). Eventually, the matrix condition number reaches a point that is too large for the computer machine precision to handle, after which the solution becomes unstable. Numerical studies presented herein indicate that the instabil-

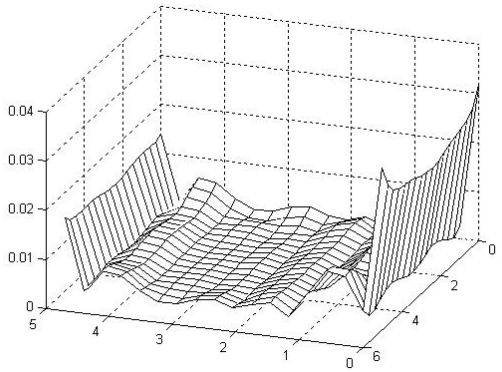

(a)

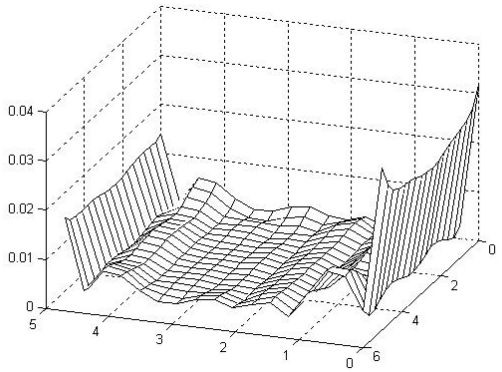

(b)

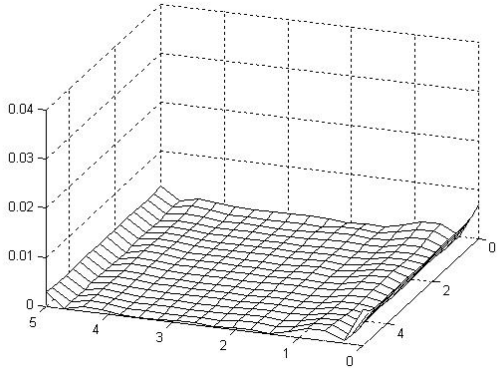

(c)

Figure 4: Error distribution in $\sigma_{xx}$ interpolation, adaptive scheme, test problem 1; (a) original solution; (b) adaptive h-scheme; (c) adaptive c-scheme

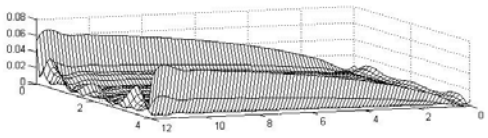

(a)

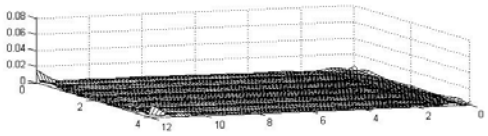

(b)

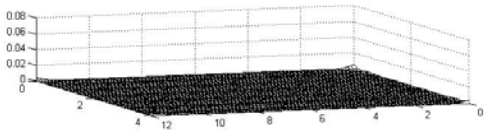

(c)

Figure 5: Error distribution in $\sigma_{xy}$ interpolation, adaptive scheme, test problem 2; (a) original solution; (b) adaptive h-scheme; (c) adaptive c-scheme

ity appears in the solution after the condition number exceeds a certain limit of 1E+16. This can be explained by the fact that the exponent of the condition number indicates the number of decimal places that the computer can lose due to round-off errors and that the double precision numbers that are used in numerical calculations on personal computers have about 16 decimal digits of accuracy. The proposed treatment scheme for improving accuracy of stress field on the boundary usually increases the ill-conditioning of equation systems. Because of this ill-conditioning, there have been doubts about the ability of standard linear equation solvers such as Gaussian elimination to solve accurately the equation systems of RBF collocation method. So, the treatment schemes should be accompanied by a stable solver to overcome the instabilities arising from round-off errors. In the next section, we briefly introduce an improved numerical solver for avoiding inaccurate computation in severely ill-conditioned systems.

## 4 Improved truncated singular value decomposition

Consider an equation system in the form of

$$\mathbf{A}\alpha=\mathbf{b}\ . \tag{20}$$

Consider the well-known singular value decomposition algorithm for a square N × N matrix, **A**, that can be decomposed as:

$$\mathbf{A}=\mathbf{V}\Sigma\mathbf{U}^T \tag{21}$$

The inverse of **A** is:

$$\mathbf{A^{-1}}=\mathbf{U}\Sigma^{-1}\mathbf{V}^{\mathrm{T}} \tag{22}$$

where $\mathbf{V}=[\mathbf{V}_1,\mathbf{V}_2,\ldots,\mathbf{V}_N]$, and $\mathbf{U}=[\mathbf{U}_1,\mathbf{U}_2,\ldots,\mathbf{U}_N]$ are orthonormal matrices with column vectors called left and right singular vectors, respectively, and Σ is a diagonal matrix of the singular values in descending order: $\sigma_1 \geq \sigma_2 \geq \ldots \geq \sigma_N > 0$. The ratio of the largest singular value to the smallest singular value gives the absolute condition number of the matrix **A**,

$$\kappa_{\mathrm{abs}}(\mathbf{A})=\frac{\sigma_1}{\sigma_N}=\|\mathbf{A}\|\cdot\|\mathbf{A}^{-1}\| \tag{23}$$

The condition number determines the loss in precision due to round-off errors and can be used to estimate the accuracy of results obtained from matrix inversion and linear equation solutions. The weak point of the SVD method is the inaccurate computation of the small singular values. For an ill conditioned matrix equation the SVD solution is dominated by contributions from small singular values, and therefore it may become unbounded and oscillatory. Hence, to mitigate the ill conditioning, one often drops all terms with $\sigma_k < \mu$ for some pre-assigned value of $\mu$, where k < N, and $\mu$ is the cut-off regularization parameter. The Hensen (1987) truncated SVD (TSVD) scheme uses the first k singular values, $\sigma_j$,j=1,...,k. The truncated inverse of **A** can be computed as:

$$\mathbf{A}^{-1}_{\mathrm{trunc}}=\mathbf{U}_{1:\mathrm{N},1:\mathrm{k}}\mathbf{\Sigma}^{-1}_{1:\mathrm{k}}\,(\mathbf{V}_{1:\mathrm{N},1:\mathrm{k}})^{\mathrm{T}}. \tag{24}$$

The TSVD scheme is widely used as an efficient solver for the ill-conditioned systems. However, for the RBF collocation method, solutions obtained from the TSVD method are not accurate and reliable.

Volokh and Vilnay (2000) observed that small singular values are inherent in the SVD of ill-conditioned systems and presented an algorithm to bypass the inaccurate computation of the small singular values. Their method will be summarized below.

Define matrices, $\mathbf{\Sigma 1}=\Sigma_{1:k}$, $\mathbf{U1}=\mathbf{U}_{1:N,1:k}$, $\mathbf{U2}=\mathbf{U}_{1:N,k+1:N}$, $\mathbf{V1}=\mathbf{V}_{1:N,1:k}$, $\mathbf{V2}=\mathbf{V}_{1:N,k+1:N}$, and $\mathbf{\Sigma 2}=\Sigma_{k+1:N}$. Their method uses the information contained in the *entire* SVD decomposition, but projects out the very small singular values into the null space to construct a stable scheme. They define new right and left matrices, of rank, N and k:

$$\mathbf{Unull}=\mathrm{null}(\mathbf{U1}^T),\quad \mathbf{Vnull}=\mathrm{null}(\mathbf{V1}^T) \tag{25}$$

Using the small singular values, **Σ2**, they constructed a new matrix, **C**:

$$\mathbf{C}_{\mathrm{k+1:N,k+1:N}}=(\mathbf{VnullV2})\Sigma 2(\mathbf{U2Unull})^{\mathrm{T}} \tag{26}$$

Then the complete inverse and solution vector consists of two parts:

$$\mathbf{A}^{-1}=\mathbf{A}^{-1}_{\mathrm{trunc}}+\mathbf{UnullC}^{-1}\mathbf{Vnull}\ , \tag{27}$$

$$\alpha=(\mathbf{A}^{-1}_{\mathrm{trunc}}+\mathbf{UnullC}^{-1}\mathbf{Vnull})\mathbf{b}\ . \tag{28}$$

The key property of this method is that the matrices **C** and Σ1 are well conditioned in contrast to the matrix **A**. The condition number of **C** depends upon the cutoff parameter $\mu$ and the well conditioning of **C**. So, the performance of the Volokh-Vilnay method depends upon the suitable choice of the cutoff parameter, $\mu$. In this paper, we employ a rational scheme to determine the cutoff parameter for the improved TSVD.

For a fixed machine precision, the cumulative round-off error reduces the number of accurate digits in the floating point arithmetic. The usual rule is that the exponent of the condition number indicates the number of decimal places that the computer can lose due to round-off errors. If the condition number is much greater than $\sqrt{1/\varepsilon}$

, where $\varepsilon$ is the machine precision, caution is advised for subsequent computations. For IEEE arithmetic, double precision numbers that usually used in the numerical arithmetic have about 16 decimal digits of accuracy and the machine precision is about $\varepsilon$ =2.2×10$^{16}$, so it is advisable to keep the condition number of the matrix $\Sigma$1 less than $\sqrt{1/\varepsilon}$= 6.7 ×10$^{8}$ by adjusting the cutoff parameter, $\mu$. So, instead of using a constant cutoff parameter, $\mu$=10$^{-8}$, as employed by Volokh and Vilney (2000), we used a floating cutoff parameter, $\mu$=$\sigma_1$×10$^{-8}$, so that

$$\kappa_{\text{abs}}(\Sigma\mathbf{1}) = \frac{\sigma_1}{\sigma_k} \leq \frac{\sigma_1}{\mu} \leq 10^8 . \tag{29}$$

This floating cutoff guarantees that the condition number of $\Sigma\mathbf{1}$, $\kappa_{abs}(\Sigma\mathbf{1}) \leq 10^8$, is bounded for IEEE 16 decimal digits of accuracy. In the highly ill-conditioned equation systems, very small singular values appear in matrix **C** and this matrix may also become ill-conditioned. The ill-conditioning problem of matrix **C** can be simply overcome by repeating the IT-SVD scheme on the matrix, **C**.

## 5 Numerical Examples

Here we utilize the boundary treatment scheme presented in the preceding sections for stabilizing the RBF direct collocation scheme. The efficiency of IT-SVD scheme for the stable solution of severely ill-conditioned equation systems arising from h-scheme and/or c-scheme refined elliptic PDE problems are investigated through numerical examples. All numerical codes are implemented with Matlab 7.2 and executed on a Core 2 Duo 2.0 GHz (4 MB Cache, 1G RAM) notebook computer running Windows XP Professional. The root-mean squared (RMS) error as defined in (18) is used to measure the solution accuracy.

$$.\text{RMS}= \frac{1}{\text{N}}\sqrt{\frac{\sum(\text{f}_\text{i}^\text{h} - \text{f}_\text{i}^\text{exact})^2}{\sum(\text{f}_\text{i}^\text{exact})^2}} \tag{30}$$

where $\text{f}_\text{i}^\text{h}$ and $\text{f}_\text{i}^\text{exact}$are the approximated and exact solution values at the point, $\mathbf{x}_i$, respectively.

### *5.1 Example 1. Higher Order Patch Test*

The first numerical example is a higher order patch test. A detailed description of the patch tests can be found in Zienkiewicz and Taylor (2000). A uniform distribution of 6×6 points and a constant shape parameter c=3 are used in the analysis. Figure (6) shows the distribution of 6×6 points. The exact solution for this problem with a Young's modulus (E) of unity and a Poisson's ratio, $\nu$ =0.25 is given in Eq (9).

Two distinct sets of BCs were considered in this analysis to study the dependency of solution accuracy upon the type of the imposed BCs. In the first set that we labeled as Dirichlet BC, the analytical displacements are prescribed on all boundaries. In the second set of BCs which we labeled as Neumann BCs, the analytical displacements (Dirichlet BC) are prescribed on the boundary identified by $\{\partial\Omega(\text{x,y}) \mid \text{x=0}\}$, and Neumann BCs are imposed on the reminding boundaries.

The error distribution in $\sigma_{xx}$ that is evaluated on a uniform 21×21 grid is shown in Figure (7). From this example we see that when Neumann BCs are imposed, the accuracy of solution is reduced significantly. This observed dependence of the accuracy upon the type of imposed boundary condition is believed to be related to the poor approximation of derivatives on the boundaries.

In the patch test with Neumann BCs, we want to converge to within the same tolerance as the patch test with Dirichlet BCs, that means we want the RMS ($\sigma_{xx}$) < 4.8E-4. As discussed previously, there are different schemes for converging to the specified accuracy. Among these are: (1) Uiform mesh refinement (h-scheme) or (2) Constant shape parameter incremental refinement (c-scheme). The results are summarized in Table 7. The standard Gaussian elimination (GE) and the IT-SVD schemes were used as the linear equation solver methods.

The numerical results of this example show that both the GE and IT-SVD schemes converged to the specified tolerance. The summarized results in Table 7 show that in this case, the IT-SVD solver did not show any advantage over the conventional GE solver. This is ascribed to the simple nature

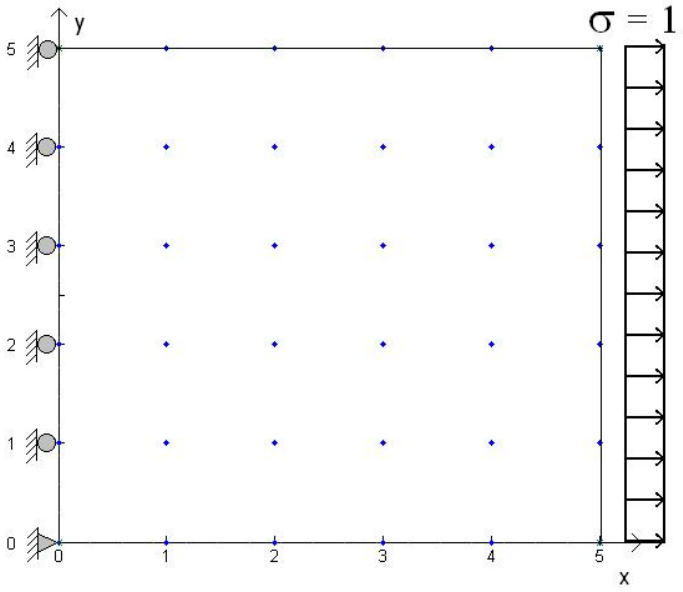


Figure 6: Regular distribution of 6×6 points in patch test problem

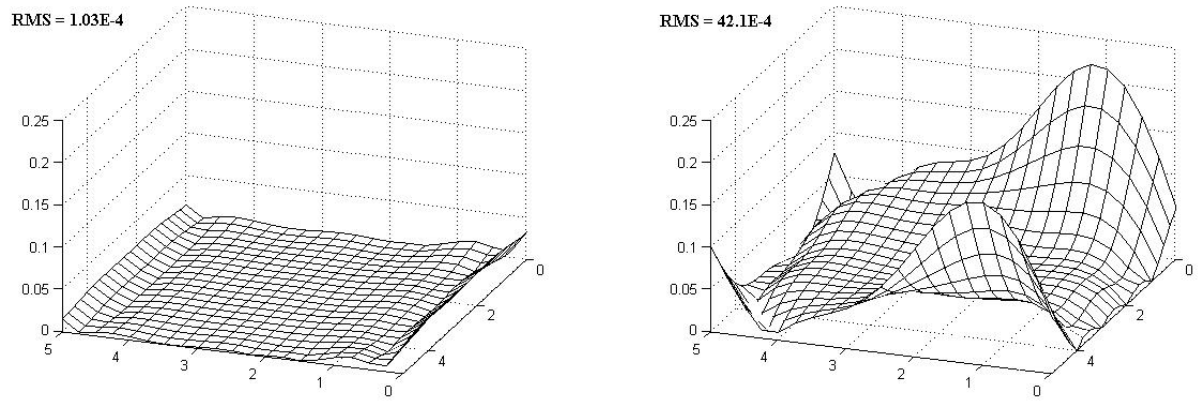


(a) (b)

Figure 7: Error distribution of in patch test problem; (a) Dirichlet BC; (b) Neumann BC

of the investigated problem that is well posed employing a low number of collocation points. So in this example, ill-conditioning is not a critical issue, and the IT-SVD method is not necessary for converging to the specified tolerance. However, this is not the case for complicated large scale physical problems requiring many collocation points, where the IT-SVD scheme should be implemented.

Nevertheless, we will point out the efficiency of the IT-SVD scheme in another way. Consider that more accurate results (namely an RMS error of $\sigma_{xx} < 1.0\text{E-}6$) are required in the patch test problem with both sets of BCs. Here again, we employed the h and c schemes to achieve the required convergence. The numerical results reveals that GE failed to converge within specified tolerance in both cases of the BCs, but the IT-SVD satisfied the criteria. In terms of CPU time and condition number of coefficient matrix, the c-scheme is more efficient than h-scheme, as depicted in Table 8.

Table 7: Numerical results for converging within the specified tolerance in patch test (RMS ($\sigma_{xx}$) <4.8E-4)

| Solver | | | GE | GE | IT-SVD | IT-SVD |
|---|---|---|---|---|---|---|
| | Data centers | c | RMS | CPU | RMS | CPU |
| Original solution | 6×6 | 3.0 | 30.906E-4 | 0.61 | 30.906E-4 | 0.68 |
| h- scheme refined | 10×10 | 3.0 | 3.5437E-4 | 2.45 | 3.5437E-4 | 2.67 |
| c-scheme refined | 6×6 | 5.0 | 4.7635E-4 | 0.61 | 4.7635E-4 | 0.68 |

Table 8: Numerical results for converging within the specified tolerance in patch test using IT-SVD solver (RMS ($\sigma_{xx}$) <1.0E-6)

| Solver | | | | | GE | GE | IT-SVD | IT-SVD |
|---|---|---|---|---|---|---|---|---|
| Problem type | Scheme | Points | c | $\log_{10}$(cond) | RMS | CPU | RMS | CPU |
| Neumann B.C | h-scheme | 25×25 | 3.0 | 20.2 | * | - | 4.2276E-7 | 87.2 |
| Neumann B.C | c-scheme | 6×6 | 16.2 | 18.0 | * | - | 8.8770E-7 | 0.65 |
| Dirichlet B.C. | h-scheme | 25×25 | 3.0 | 20.1 | * | - | 6.2373E-7 | 27.6 |
| Dirichlet B.C. | c-scheme | 6×6 | 16.2 | 15.3 | * | - | 9.6454E-7 | 0.70 |

* The method failed to converge within the specified tolerance

The convergence rate is also studied in the patch test problem. Uniformly distributed sets of 3×3, 6×6, 11×11and 21×21 collocation points are used for this purpose. The second set of BCs were employed in the convergence analysis. The resulting equation systems of the RBF direct collocation method were solved by the standard Gaussian elimination (GE) and the IT-SVD scheme. The shape parameters were taken to be c=3 and c=10. Figure (8) shows that in the case of c=3, by refining the mesh size h up to 11×11 points, the GE converges to exact solution. Numerical instability was observed when the number of collocation points was increased beyond 11×11 points. The ill-conditioning problem limits the maximum attainable accuracy. As shown in Figure (8), the numerical instability arising from GE is dominant whenever the coefficient matrix condition number becomes larger than $10^{12}$. In contrast, the IT-SVD method is still stable and converges to exact solution even in highly ill-conditioned equation systems.

Increasing the shape parameter usually improves the convergence rate of the solutions. Despite of the improved convergence rate, Figure (8) shows that increasing the shape parameter up to c=10 resulted in highly ill-conditioned systems and GE solution becomes unstable when more than 6×6 points were used. Nevertheless, the IT-SVD is still stable and the results converge to the exact solution. Utilizing larger values of MQ shape parameter together with the IT-SVD solver increases the convergence rate and makes it possible to achieve stable and superiorly accurate solutions.

### 5.2 Example 2. Cantilever Beam

A cantilever beam subjected to tip shear traction is the second example that we examine to demonstrate the efficiency of the h and/or c scheme refinement together with the IT-SVD solver. Figure (9) shows the geometry of the cantilever beam as well as the distribution of collocation points used in this analysis. A regular distribution of 31×11 points in the domain and a constant shape parameter c=2 are used in the analysis. The length and height of beam are L=12 and D=4, respectively. The plane stress condition is assumed in the analysis with the mechanical properties of E=1000 and $\nu$=1/3.The analytical solutions of this problem are given in Eq (16-18).

$$.\partial\Omega_1: \quad \{x=0, 0 \le y \le D\}, \quad u_x = \frac{-P}{6EI}(y-D/2)[(2+\nu)y(y-D)] \tag{31}$$

$$.\partial\Omega_1: \quad \{x=0, 0 \le y \le D\}, \quad u_y = \frac{(P\nu L)}{2EI}(y-D/2)^2 \tag{32}$$

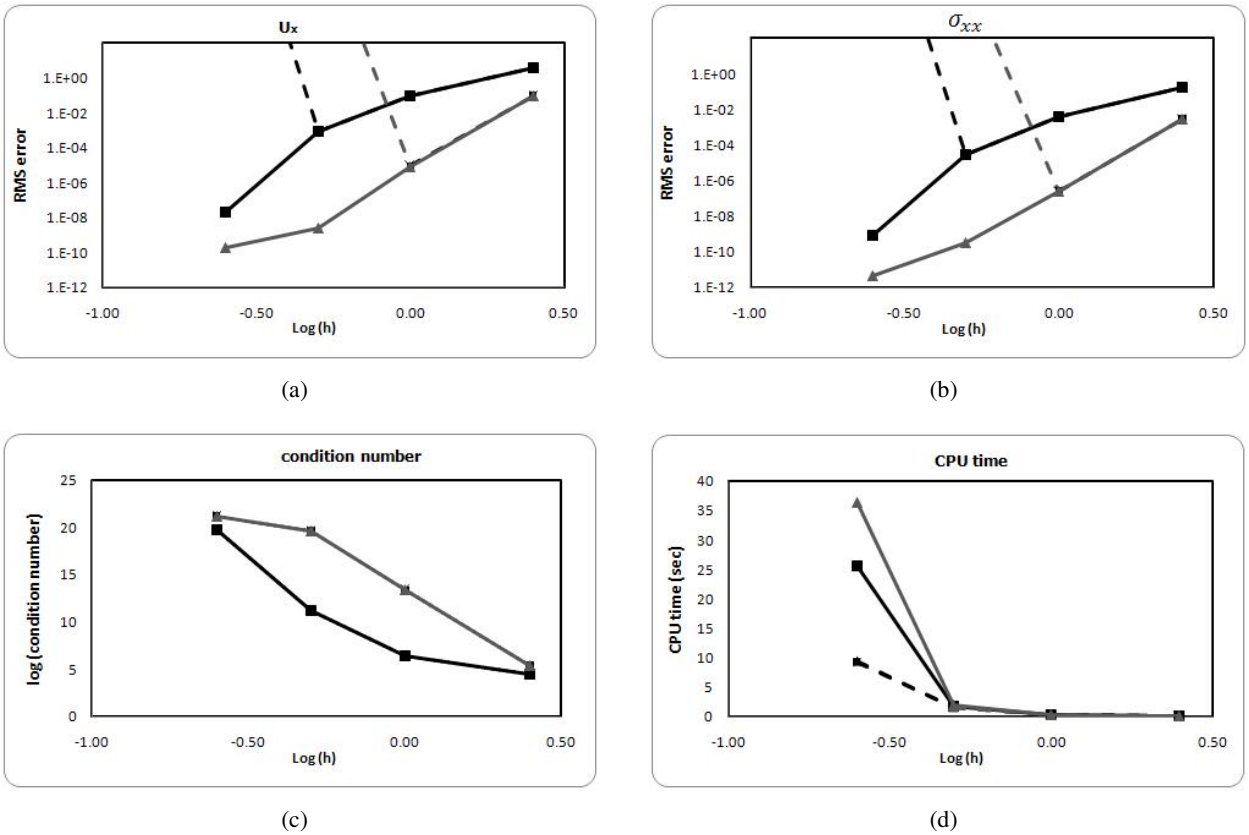


Figure 8: Convergence rate in patch test (a) displacement $u_x$; (b) stress $\sigma_{xx}$ ; (c) condition number of coefficient matrix; (d) CPU time

$$.\partial\Omega_2\text{: } \{x=L, 0 \leq y \leq D\},\ .t_x = 0,\ t_y = \frac{Py}{2I}(y-D) \tag{33}$$

$$\partial\Omega_{3,4}\text{:}\{0<x<D,\ y=0,D\}\ .t_x = 0,\ t_y = 0. \tag{34}$$

We solve this problem for two distinct sets of boundary conditions labeled as Dirichlet BC and Neumann BC, respectively. In the first set labeled as Dirichlet BC, the displacements given by Eqs (16-17) are applied at all boundary nodes. The Neumann condition is inserted in the second set of boundary condition where the displacement is applied at boundary $\partial\Omega_1$ and the traction at the remainder boundary nodes, as stated in Eq (30-33).

The errors distribution and the corresponding RMS error estimations calculated on uniform distribution of $61\times21$ approximation points are shown in Figure (10).

Figure (10) shows that the solution of cantilever beam problem with Dirichlet BC holds the admissible accuracy (RMS=3.9E-4). In contrast to the results of the cantilever beam problem with Dirichlet BCs, considerable error appears in the solution when Neumann BC are imposed, (RMS=1.1E-1). This large error with Neumann BCs is mainly attributed to the poor accuracy of the stress field approximation on the boundary and to the severely ill-conditioned equation system of the cantilever beam problem that magnifies the errors. In this case, one should implement the h and/or c refinement scheme to improve the accuracy of approximation together with the IT-SVD to overcome the ill-conditioning problems to converge within desired accuracy.

Here again in the problem with Neumann BCs, we desire to converge to within the same tolerance as the problem with Dirichlet BCs, namely RMS $(\sigma_{xx}) < 3.9\text{E-}4$. Table 9 shows the IT-SVD method and its corresponding CPU time required for converging to the specified tolerance. This re-

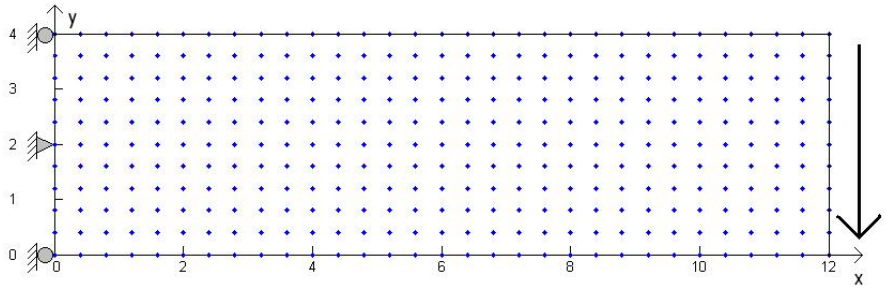


Figure 9: Regular distribution of 31×11 points in cantilever beam problem

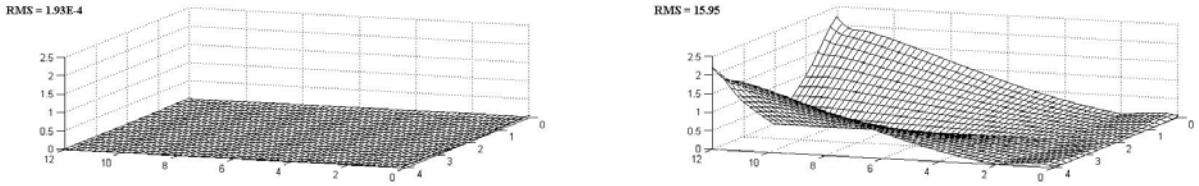


(a) (b)

Figure 10: Error distribution of $\sigma_{xx}$ in cantilever beam problem; (a) Dirichlet BC; (b) Neumann BC

Table 9: Numerical results for converging the solution of cantilever beam problem to the specified tolerance (RMS ($\sigma_{xx}$) <3.9E-4)

| Solver | Data centers | c | GE RMS | GE CPU | IT-SVD RMS | IT-SVD CPU |
|---|---|---|---|---|---|---|
| Original solution | 31×11 | 2 | 1.1160E-1 | 12.9 | 1.1160E-1 | 19.5 |
| c-scheme refined | 31×11 | 5.1 | * | - | 3.3233E-4 | 19.5 |

* The method failed to converge within specified tolerance

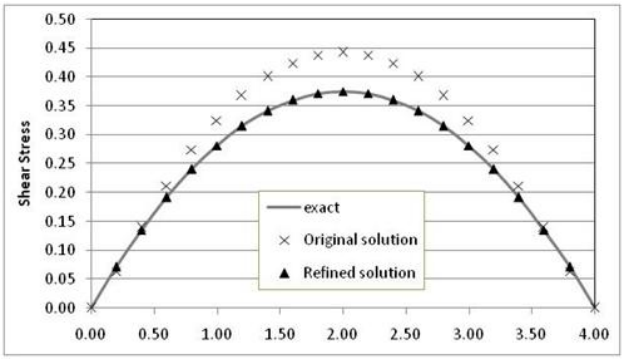


Figure 11: Shear stress at section x=L/2 of the beam

Table 10: RMS and $L_\infty$ error norms in finely tuned cantilever beam problem

| Variable | RMS | $L_\infty$ |
|---|---|---|
| $u_x$ | 1.8277E-4 | 3.9581E-6 |
| $u_y$ | 7.0199E-5 | 1.4576E-6 |
| $\sigma_{xx}$ | 1.0978E-6 | 8.8429E-6 |
| $\sigma_{xy}$ | 1.1235E-7 | 1.6266E-6 |

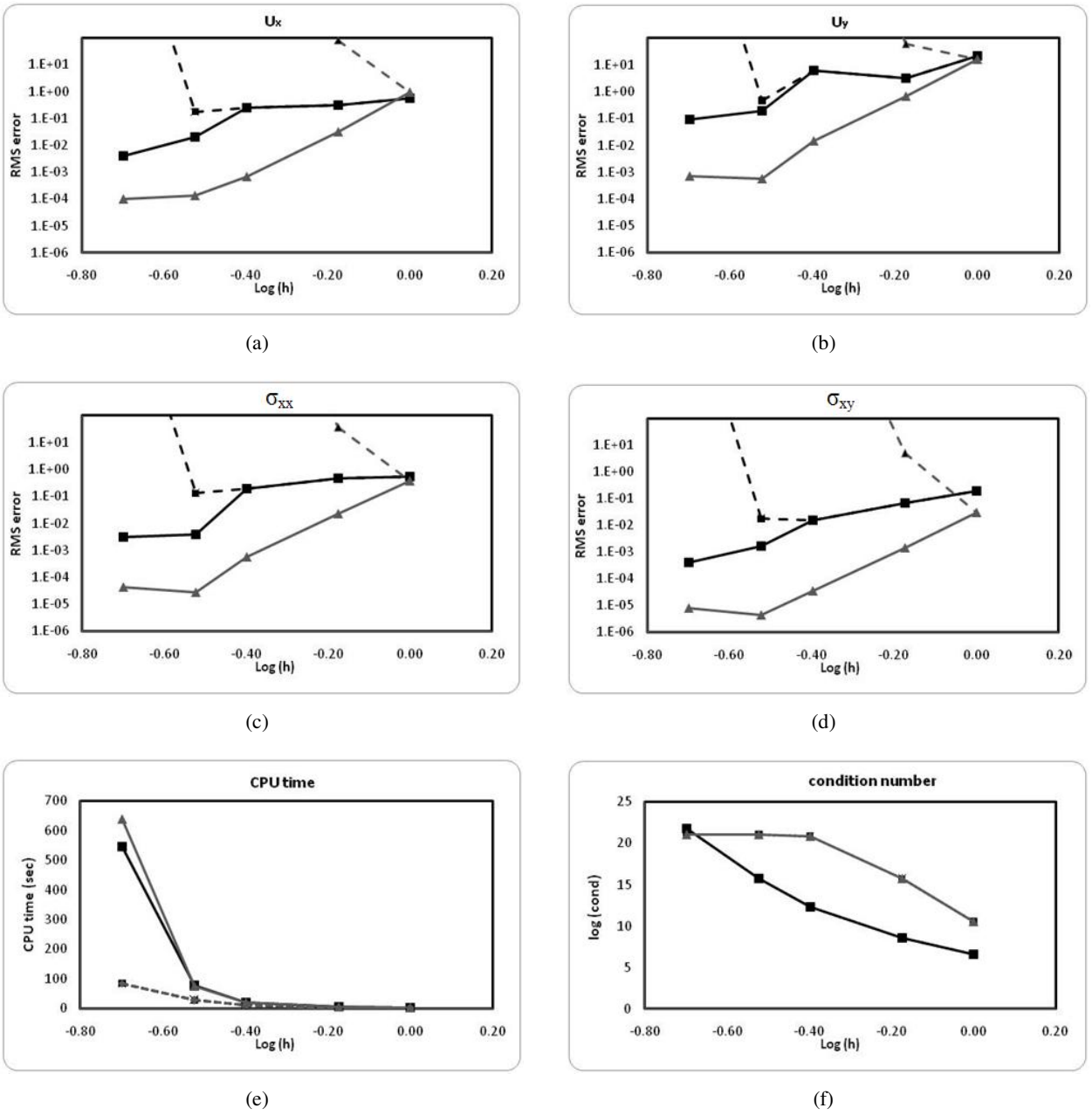


Figure 12: Convergence rate in cantilever beam problem with uniformly distributed nodes (a) displacement $u_x$; (b) displacement $u_y$; (c) stress $\sigma_{xx}$; (d) stress $\sigma_{xy}$; (e) condition number of coefficient matrix; (f) CPU time

sults shows that GE failed to converge within desired tolerance, but the IT-SVD fulfilled the criteria.

Figure (11) shows the comparison between the shear stress at the section of x=L/2 calculated analytically and numerically. It is clearly shown that the solutions refined with c-scheme and stabilized by IT-SVD are much more accurate than original solutions.

The convergence rates were also examined using five different arrangements of uniformly distributed points: $13\times5$, $19\times7$, $31\times11$, $41\times15$, and $61\times21$ nodes. Neumann BCs as stated in Eq (21),

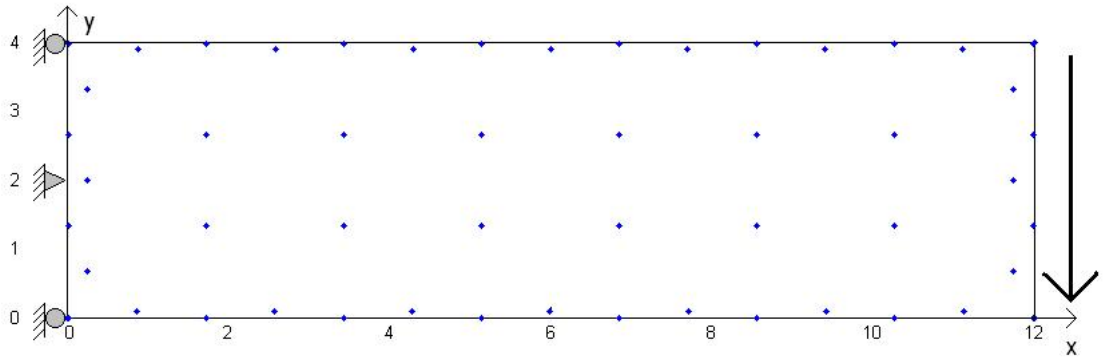


Figure 13: Adaptive distribution of 52 points in cantilever beam problem

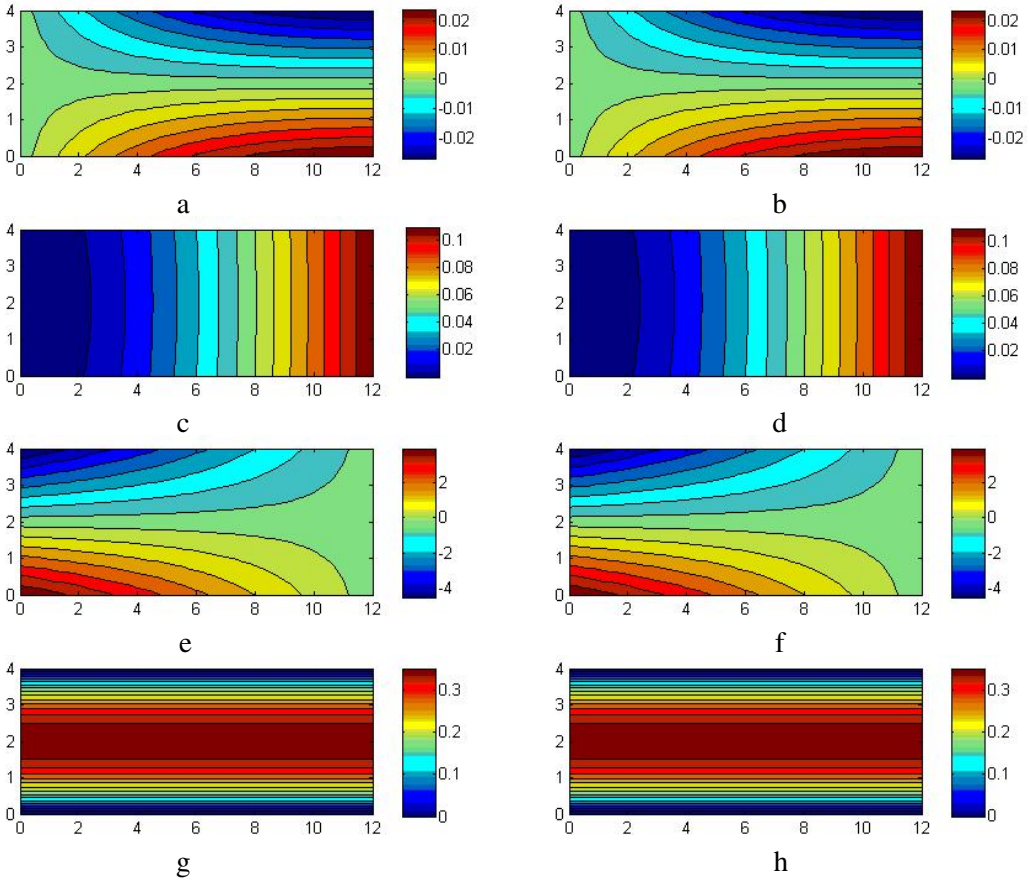


Figure 14: The exact and the calculated solution of the cantilever beam problem (a) exact displacement $u_x$; (b) calculated displacement $u_x$; (c) exact displacement $u_y$; (d) calculated displacement $u_y$; (e) exact stress $\sigma_{xx}$; (f) calculated stress $\sigma_{xx}$; (g) exact stress $\sigma_{xy}$; (h) calculated stress $\sigma_{xy}$

were imposed in the analysis. Two shape parameters, c=2 and c=6, were used in separate simulations.

Figure (12) shows RMS norms of the results. Similar to the previous case, the IT-SVD solver shows excellent stability and convergence properties, while the standard GE solver displays both numerical instability and a deterioration of accuracy on successively finer nodal distributions.

When the c-scheme with c=6 was employed, the convergence rate of the results with the IT-SVD also improved significantly.

Despite the sensitivity of the RBF collocation method to the Neumann type BCs, we would like to demonstrate that even with a smaller number of collocation points, good accuracy can be achieved. Both the adaptive mesh refinement and adaptive shape parameter increment were employed in the cantilever beam problem with Neumann BCs and the resulting equation systems were solved by the IT-SVD scheme. The adaptive distribution of 52 (= (4×8)+20) points as shown in Figure (13) was used in the analysis. The interior and boundary shape parameter was selected as $c_{\Omega\setminus\partial\Omega}$=50 and $c_{\partial\Omega}$= 75, respectively. Besides the RMS error, the $L_\infty$ norm was also used to evaluate accuracy of the solution.

The exact and the calculated displacement and stress field of a cantilever beam problem are shown in Figure (14). The RMS and $L_\infty$ error norms that are summarized in Table 10 shows that accurate solutions can be achieved by combining the adaptive schemes with the IT-SVD solver even for semi large scale and instable problems such as cantilever beam subjected to Neumann BCs.

## 6 Concluding remarks

Meshfree methods based on MQ-RBF collocation are investigated in this paper. We show numerically that the direct MQ-RBF collocation method leads to significant error in solving PDEs with Neumann BCs since the spatial derivatives are poorly approximated on the natural boundary. Hence, two treatment schemes namely the c-scheme and h-scheme were proposed to improve the accuracy of the approximation near and on the boundary. Numerical results show that both the c-scheme and h-schemes significantly increase the ill-conditioning of the equation systems that causes numerical instability in the solution. To mitigate the ill-conditioning problems arising from the h-and c-schemes, the IT- SVD scheme was utilized for the solution of the linear equation systems. The c-scheme and h-scheme treatment methods together with IT-SVD solver have been applied successfully to solve the two-dimensional elasticity problems described by the Navier's equation.

The h-scheme increases the rank of the coefficient matrix that leads to an increased expense in computer storage and CPU time, while the c-scheme is performed without extra CPU cost or storage. So the c-scheme is preferable to the h-scheme. In addition, the adaptive schemes are superior and more desirable over uniform schemes for the solution of PDE problems especially those with high gradients in local regions. The robustness of combined adaptive c-h scheme together with IT-SVD solver was demonstrated through a numerical example where the values of maximum error norms were in the were in the order of $10^{-6}$. Most of engineering problems do not require RMS or $L_\infty$ errors on the accuracy order of $10^{-6}$ . However it is shown that, much more complicated problems can be solved accurately by RBF collocation methods employing the IT-SVD scheme presented herein. Some authors have claimed that RBFs could not be extended to complicated, multi-dimensional PDE problems. Nevertheless, we will combine the h-anc c-schemes with the IT-SVD solver with the domain decomposition method for the solution of complicated large scale engineering problems. In a future paper, we intend to demonstrate this accelerated convergence with variable shape parameters with the IT-SVD. We will show that the implementation of the IT-SVD is capable of achieving superior stable results with large and adaptively tuned values of variable shape parameter, $c_j^2$.

## References

**Adibi, H; Es.haghi, J.** (2007): Numerical solution for biharmonic equation using multi- level radial basis functions and domain decomposition methods. *Appl Math Comput*., Vol. 186, pp.246-255.

**Buhmann, M.D.; Micchelli, C.A**. (1990): Multivariate interpolation in odd-dimensional

Euclidean spaces using multiquadrics, *Constr. Approx.* Vol. 6(12) , pp.21-34.

**Cheng, A. H. D.; Golberg, M.A.; Kansa, E. J.;**

**Zammito, T.** (2003): Exponential convergence and h-c multiquadric collocation method for partial differential equations, *Num. Meth. PDEs*. Vol. 19, pp.571-594.

**Emdadi, A.; Kansa, E.J.; Libre, N.A.; Rahimian, M.; Shekarchi, M.** (2007): (submitted for publication): Stable PDE solution methods for large Multiquadric shape parameters, *CMES: Computer Modeling in Engineering Sciences.*

**Fedoseyev, A.I.; Friedman, M.J.; Kansa, E.J.** (2002): Improved multiquadric method for elliptic partial differential equations via PDE collocation on the boundary, *Comput. Math. Appl.,* Vol. 43(3-5) , pp. 491-500.

**Ferreira, A.J.M; Roque, C.M.C.; Jorge, P.M.N : Kansa, E.J**. (2005): Static deformations and vibrational analysis and sandwich plates using a layerwise theory and multiquadric discretization, *Eng. Anal. Bound. Elem.* Vol. 29 , pp. 1104-1114.

**Fornberg, B.; Driscoll, T.A**. (2002): Interpolation in the limit of increasingly .at radial

basis functions, *Comput. Math. Appl*, Vol. 43(3.5) , pp.413-421.

**Fornberg , B; Wright, G**.(2004): Stable computation of multiquadric interpolants for all values of the shape parameter, *Comput. Math. Appl*, Vol. 48 (5-6), pp. 853-867.

**Fornberg, B; Wright, G; Larsson, E.** (2004): Some observations regarding interpolants in the limit of flat radial basis functions, *Comput Math Appl*. Vol. 47, pp. 37-55.

**Hansen, P.C.** (1987): The truncated SVD as a method for regularization, *BIT*, Vol. 27, pp. 534-553.

**Hardy, R.L.** (1971): Multiquadric equations of topography and other irregular surfaces, *J. Geo-Phys. Res.* Vol. 176, pp. 1905-1915.

**Hardy, R.L.** (1990): Theory and application of the multiquadric-biharmonic method: 20 years of discovery, *Comput. Math. Appl.*,Vol. 19(6-8), pp.163-208.

**Hu, H.Y.; Chen, J.S.; Hu, W.** (2006): Weighted radial basis collocation method for boundary value problems, *Int. J. Numer. Meth. Eng.* Vol. 69, pp. 2736-2755.

**Huang, C.-S.; Lee, C.-F. ; Cheng, A.H.-D.** (2007): Error estimate, optimal shape parameter and high precision computation of multiquadric collocation method, *Eng. Anal. Bound. Elem.* Vol. 31, pp.615-623.

**Ingber, M.S. ; Chen, C.S.; Tanski, J.A.** (2004): A mesh free approach using radial basis functions and parallel domain decomposition for solving three dimensional diffusion equations, *Int. J. Num. Meth. Eng.*, Vol. 60, pp.2183-2201.

**Kansa, E.J.; Hon, Y.C.** (2000): Circumventing the ill-conditioning problem with multiquadric radial basis functions: Applications to elliptic partial differential equations, *Comput. Math. Applic.*, Vol. 39 (7/8) , pp. 123-137.

**Libre, N.A.; Emdadi, A.; Rahimian, M.; Shekarchi, M.** (2006): Investigation of the Use of Radial Basis Functions Method for Solving static Problems, *The Eighth Int. Conf. on Computational Structures Technology*, Las Palmas de Gran Canaria, Spain.

**Ling, L.; Kansa, E.J.** (2004): Preconditioning for radial basis functions with domain decomposition, *Math. Comput. Model.*, Vol. 40, pp.1413-1427.

**Liu, G.R.; Gu, Y.T.** (2003): A meshfree method: meshfree weak-strong (MWS) form method for 2D solids, *Comput Mech.* Vol. 33, pp.2-14.

**Madych, W.R.; Nelson, S.A**. (1988): Multivariate interpolation and conditionally positive de finite functions, *Approx. Theory Applic*. Vol. 4, pp.77-89.

**Madych, W.R.; Nelson, S.A.** (1990): Multivariate interpolation and conditionally positive de finite functions, II, *Math. Comput*. Vol. 54, pp. 211-230.

**Madych, W.R**. (1992): Miscellaneous error bounds for multiquadric and related interpolators, *Comput. Math. Applic.* Vol. 24(12): pp. 121-138.

**Mai-Duy, N.; Tran-Cong, T.** (2003): Approximation of function and its derivatives using radial basis function networks, *Appl Math Modeling*, Vol. 27, pp.197-220.

**Mai-Duy, N; Tran-Cong, T**. (2007): Solving Partial differential Equations With Point Collocation And One-Dimensional Integrated Interpolation Schemes, *ICCES*, vol.3, no.3, pp.127-132.

**Mai-Duy, N; Khennane, A.; Tran-Cong, T**. (2006): Computation of Laminated Composite Plates using Integrated Radial Basis Function Networks, *CMC: Computers, Materials, and Continua*, Vol. 5, No. 1, pp. 63-78.

**Micchelli, C.A.** (1986): Interpolation of scattered data: distance matrices and conditionally positive definite functions, *Constr. Approx.* Vol. 2, pp. 11-22.

**Sarler, B.** (2005): A Radial Basis Function Collocation Approach in Computational Fluid Dynamics, *CMES: Computer Modeling in Engineering & Sciences,* Vol. 7, No. 2, pp. 185-194.

**Schaback, R**. (1995): Error estimates and condition numbers for radial basis function interpolation, *Adv. Comp. Math*. Vol. 3, pp 251-264.

**Timoshenko, S.P.; Goodier, J.N**. (1970): *Theory of Elasticity*, third ed., McGraw-Hill, New York.

**Tolstykh, A.I.; Shirobokov, D.A.** (2005): Using radial basis functions in a finite difference mode, *CMES: Computer Modeling in Engineering & Sciences,* Vol. 7, No. 2, pp. 207-222.

**Volokh, K.Y.; Vilnay, O.** (2000): Pin-pointing solution of ill-conditioned square systems of linear equations, *Appl. Math. Lett.* Vol. 13, pp.119-124.

**Wen, P.H. ; Hon, Y.C.** (2007): Geometrically Nonlinear Analysis of Reissner-Mindlin Plate by Meshless Computation, *CMES: Computer Modeling in Engineering & Sciences*, Vol. 21, No. 3, pp. 177-192

**Wendland, H.** (2005): *Scattered Data Approximation*, Cambridge University Press, Cambridge.

**Wertz, J.; Kansa, E.J.; Ling, L.** (2006): The role of the Multiquadric Shape Parameters in solving Elliptic Partial differential Equations, *Comput. Math. Applic.* Vol. 51(8), pp. 1335-1348.

**Young, D.L.; Chen, C.S.; Wong, T.K.** (2005): Solution of Maxwell's Equations Using the MQ Method, *CMC: Computers, Materials and Continua*, Vol. 2, No. 4, pp. 267-276

**Zienkiewicz, O.C.; Taylor, R.L**. (2000): *The finite element method*, Vol. 1, 5th Ed. Butterworth-Heinemann, Oxford.

**Zhang, X.; Song, K.Z.; Lu, M.W; Liu, X.H.** (2000): Meshless methods based on collocation with radial basis functions, *Comput Mech*. Vol. 26, pp. 333-343.